Exploring the genetic diversity of the Japanese Population: Insights from a Large-Scale Whole Genome Sequencing Analysis

Yosuke Kawai,[1,*] Yusuke Watanabe,[1,#a] Yosuke Omae,[1,2] Reiko Miyahara,[2,#b] Seik-Soon Khor,[1] Eisei Noiri,[2] Koji Kitajima,[2,3] Hideyuki Shimanuki,[2,3] Hiroyuki Gatanaga,[4] Kenichiro Hata,[5] Kotaro Hattori,[6] Aritoshi Iida,[7] Hatsue Ishibashi-Ueda,[8] Tadashi Kaname,[9] Tatsuya Kanto,[10] Ryo Matsumura,[6] Kengo Miyo,[11] Michio Noguchi,[8] Kouichi Ozaki,[12,13] Masaya Sugiyama,[14] Ayako Takahashi,[8] Haruhiko Tokuda,[12,15,16] Tsutomu Tomita,[8] Akihiro Umezawa,[17] Hiroshi Watanabe,[12,18] Sumiko Yoshida,[6] Yu-ichi Goto,[19] Yutaka Maruoka,[20] Yoichi Matsubara,[21] Shumpei Niida,[12] Masashi Mizokami,[15] and Katsushi Tokunaga[1,2,*]

[1] Genome Medical Science Project, Research Institute, National Center for Global Health and Medicine, Shinjuku-ku, Tokyo 162-8655, Japan

[2] Central Biobank, National Center Biobank Network, Shinjuku-ku, Tokyo 162-8655, Japan

[3] Department of Data Science Center for Clinical Sciences, National Center for Global Health and Medicine, Shinjuku-ku, Tokyo 162-8655, Japan

[4] AIDS Clinical Center, National Center for Global Health and Medicine, Shinjuku-ku, Tokyo 162-8655, Japan

[5] Department of Maternal-Fetal Biology, National Center for Child Health and Development, Setagaya-ku, Tokyo 157-8535, Japan

21 [6] Department of Bioresources, Medical Genome Center, National Center of Neurology and
22 Psychiatry, Kodaira, Tokyo 187-8551, Japan
23 [7] Department of Clinical Genome Analysis, Medical Genome Center, National Center of
24 Neurology and Psychiatry, Kodaira, Tokyo 187-8551, Japan
25 [8] NCVC Biobank, National Cerebral and Cardiovascular Center, Suita, Osaka 564-8565,
26 Japan
27 [9] Department of Genome Medicine, National Center for Child Health and Development,
28 Setagaya-ku, Tokyo 157-8535, Japan
29 [10] Department of Liver Disease, Research Center for Hepatitis and Immunology, National
30 Center for Global Health and Medicine, Ichikawa, Chiba 272-8516, Japan
31 [11] Center for Medical Informatics and Intelligence, National Center for Global Health and
32 Medicine, Shinjuku-ku, Tokyo 162-8655, Japan
33 [12] Medical Genome Center, Research Institute, National Center for Geriatrics and
34 Gerontology, Obu, Aichi 474-8511, Japan
35 [13] RIKEN Center for Integrative Medical Sciences, Yokohama, Kanagawa 230-0045, Japan
36 [14] Genome Medical Sciences Project, Research Institute, National Center for Global Health
37 and Medicine, Ichikawa, Chiba 272-8516, Japan
38 [15] Department of Metabolic Research, Research Institute, National Center for Geriatrics and
39 Gerontology, Obu, Aichi 474-8511, Japan
40 [16] Department of Clinical Laboratory, Hospital, National Center for Geriatrics and
41 Gerontology, Obu, Aichi 474-8511, Japan

42 [17] Center for Regenerative Medicine, National Center for Child Health and Development,
43 Setagaya-ku, Tokyo 157-8535, Japan
44 [18] Innovation Center for Translational Research, Hospital, National Center for Geriatrics
45 and Gerontology, Obu, Aichi 474-8511, Japan
46 [19] Medical Genome Center, National Center of Neurology and Psychiatry, Kodaira, Tokyo
47 187-8551, Japan
48 [20] Department of Oral and Maxillofacial Surgery, National Center for Global Health and
49 Medicine, Shinjuku-ku, Tokyo 162-8655, Japan
50 [21] Executive Officer, National Center for Child Health and Development, Setagaya-ku,
51 Tokyo 157-8535, Japan
52 [#a] Present address: Department of Biological Sciences, Graduate School of Science, The
53 University of Tokyo, Bunkyo-ku, Tokyo 113-8654, Japan
54 [#b] Present address: Center for Surveillance, Immunization and Epidemiologic Research,
55 National Institute of Infectious Diseases, Shinjuku-ku, Tokyo 162-8640, Japan
56

57 *Corresponding authors

58 Email: ykawai@ri.ncgm.go.jp (Y.K.); katokunaga@ri.ncgm.go.jp (K.T.)

59 **Short title:** Genomic variation characterization of ancestry in Japan

60

Abstract

The Japanese archipelago is a terminal location for human migration, and the contemporary Japanese people represent a unique population whose genomic diversity has been shaped by multiple migrations from Eurasia. Through high-coverage whole-genome sequencing (WGS) analysis of 9,850 samples from the National Center Biobank Network, we analyzed the genomic characteristics that define the genetic makeup of the modern Japanese population from a population genetics perspective. The dataset comprised populations from the Ryukyu Islands and other parts of the Japanese archipelago (Hondo). Low frequency detrimental or pathogenic variants were found in these populations. The Hondo population underwent two episodes of population decline during the Jomon period, corresponding to the Late Neolithic, and the Edo period, corresponding to the Early Modern era, while the Ryukyu population experienced a population decline during the shell midden period of the Late Neolithic in this region. Genes related to alcohol and lipid metabolism were affected by positive natural selection. Two genes related to alcohol metabolism were found to be 12,500 years out of phase with the time when they began to be affected by positive natural selection; this finding indicates that the genomic diversity of Japanese people has been shaped by events closely related to agriculture and food production.

Author summary

The human population in the Japanese archipelago exhibits significant genetic diversity, with the Ryukyu Islands and other parts of the archipelago (Hondo) having undergone distinct evolutionary paths that have contributed to the genetic divergence of the populations in each region. In this study, whole genome sequencing of healthy individuals from national research hospital biobanks was utilized to investigate the genetic diversity of the Japanese population. Haplotypes were inferred from the genomic data, and a thorough population genetic analysis was conducted. The results indicated not only genetic differentiation between Hondo and the Ryukyu Islands, but also marked differences in past population size. In addition, gene genealogies were inferred from the haplotypes, and the patterns were scrutinized for evidence of natural selection. This analysis revealed unique traces of natural selection in East Asian populations, many of which were believed to be linked to dietary changes brought about by agriculture and food production.

Introduction

The Japanese archipelago is located in the eastern part of the Eurasian continent and is one of the final destinations of the human migration out of Africa. While the identity of the first human groups to reach the Japanese archipelago is uncertain, the Jomon people, who were hunter-gatherers known for their pottery, lived in the region after 16,000 years ago. The genetic diversity of the peoples of the Japanese archipelago underwent a dramatic transformation following the Yayoi Period, which began around 3,000 years ago with the migration of agriculturalists from Eurasia. Genome analysis of ancient and modern humans has shown that they admixed with the originally inhabited Jomon people, resulting in the genetic diversity of the modern Japanese population from the Yayoi people. This process is thought to have started on Kyushu Island and then gradually spread throughout the archipelago. Although the Ryukyu Islands are separated from Kyushu Island by a significant distance, the agricultural culture known as the Gusuku period began 800 years ago, and it is believed that this agriculture was introduced by migrants from the mainland. These long histories of migration and admixture have shaped the genetic diversity of the peoples of the Japanese archipelago. Previous genome analyses have attempted to reveal this genetic diversity, but most have only sampled specific regions and therefore have been insufficient to fully examine the genetic diversity of the Japanese archipelago as a whole. In this study, we used whole-genome sequencing data from subjects from a wide range of regions in the Japanese archipelago to more fully understand the genetic diversity of the peoples of the archipelago.

120 There are six national research hospitals in Japan that specialize in advanced medical care
121 and research, and each of them maintains its own biobank that collects and stores biological
122 samples from patients. National Center Biobank Network (NCBN) is a federation of these
123 centers that collaborate to provide samples, genomic and clinical information, and public
124 relations. In this study, we performed WGS of 9,850 individual DNA specimens stored in
125 the biobanks of NCBN. These biobanks are located in three distinct regions of Japan:
126 NCGM, NCCHD, and NCNP in the Tokyo area; NCGG in Aichi Prefecture in the central
127 area in the Honshu Island; and NCVC in Osaka Prefecture in the western area in Honshu
128 Island. Therefore, the genomic information obtained in the present study is expected to
129 reflect the regional diversity of Japan to some extent. Here, we characterized the data
130 obtained from this analysis and described the genetic diversity in the Japanese population.

131 Results

132 Whole genome sequencing analysis

133 DNA samples from 9,850 individuals from five National Center Biobanks were analyzed
134 using WGS, and the data in FASTQ format were received from the outsourced laboratory.
135 The received data were processed through the primary data analysis pipeline to obtain
136 mapping results and variant call results. Quality control (QC) metrices were calculated to
137 confirm that stable quality analysis was obtained (Fig 1). The autosomes had an average
138 read depth of 34.0 ± 2.4, and the average insert length of the reads was 703 +/- 30 bp. The
139 mapping rate per sample was 99.99% ± 0.39%. These statistics did not vary significantly

140 between samples, and there was no clear bias between biobanks except for saliva samples.
141 The saliva samples showed lower mapping rates than the blood samples, probably due to
142 the foreign DNA in the saliva.

143 Summary and accuracy of SNP and short insertion and 144 deletions

145 Variants were characterized by joint calling to integrate individual variant information. In
146 this analysis, we performed joint calling of the gVCFs of 9,287 samples from NCBN,
147 analyzed at the time of writing, together with 2,504 samples from the International 1000
148 Genomes project (S1 Table). The VCF obtained after the joint call contained a total of
149 208,785,859 records, of which 88.5% (184,864,563) passed the filtering using Variant
150 Quality Score Recalibration (VQSR). We found 122,459,307 variants after focusing only
151 on the variants in the NCBN samples, and 86.3% (105,729,588) of them passed the filter of
152 VQSR. Of the variants that passed the filter, 87,246,166 were single nucleotide variants
153 (SNVs) and 18,483,422 were short insertion and deletions (INDELs); 47% (41,046,547) of
154 the SNVs and 39.8% (7,361,318) of the INDELs that passed the filter were novel variants
155 not registered in dbSNP151. Most of the novel variants were very rare. For example,
156 34.56% of the known SNVs were singletons found as the heterozygous genotypes of one
157 sample out of 9,287 individuals, and 86.73% were observed at a very low frequency of less
158 than 0.5%. Conversely, 67.46% of the novel variants not registered in dbSNP were
159 singletons, and the percentage of SNVs with a frequency less than 0.5% was more than

160 99.99%. This is consistent with previous reports that most novel variants are found
161 privately [3–6].

162 We evaluated the accuracy of the variants using two approaches. First, we performed the
163 genotyping using SNP array to estimate the degree of genotype concordance with WGS
164 results. For this purpose, genome-wide genotyping using the SNP array on the DNA
165 samples of 448 individuals who had undergone WGS analysis was conducted. The 639,508
166 autosomal SNPs remaining after variant QC in the SNP array were compared with the
167 results obtained after WGS analysis. The number of mismatches ranged from 66 to 7,205
168 per sample, with an average of 408.7. As a result, the average discordance rate between the
169 two sets of variants was 0.063%. This estimate appears to be a conservative estimate of the
170 error, as it is primarily concentrated in a region that is easy to analyze and for which probes
171 are designed on SNP arrays. Then, we compared the genotypes of the trio samples to
172 estimate the frequency with which the offspring of a trio had heterozygous or non-reference
173 homozygous variants whose parents' genotypes did not follow the pattern expected from
174 Mendelian low. The sample analyzed in this study contained 148 trios of parents and
175 offspring. We observed the inheritance pattern of genotypes from an average of 4,284,264
176 variants per trio. Of these, 6,448.4 (0.15%) had an abnormal inheritance. This percentage
177 became more pronounced when stratified by the novelty of the variants, e.g., the known
178 SNVs and INDELs had error rates of 0.09% and 0.42%, respectively, with errors in the
179 inheritance pattern, whereas the novel SNVs and INDELs had error rates of 2.26% and
180 10.9%, respectively. The Mendelian heritability errors can include the sequencing or

181 genotyping error, *de novo* mutations, and gene conversions in the parents' gametes.
182 However, our estimates approximate the error rate of genotyping in this study.

183 Ancestry inference and allele frequency distribution

184 We conducted the principal component analysis (PCA) to identify the ancestry of NCBN
185 samples. After removing 20 samples with a call rate below 95%, Identical-by-Descent
186 (IBD) was used to detect related samples, resulting in 8,972 and 2,493 unrelated samples
187 from NCBN and the International 1000 Genomes project, respectively. PCA using these
188 samples detected 21 NCBN samples not belonging to the East Asian populations (Fig 2A).
189 Furthermore, when PCA was performed only on East Asians, the samples were divided into
190 two clusters: one consisting of continental populations (Han Chinese in Beijing; CHB, Han
191 Chinese South; CHS, Kinh Vietnamese; KHV, Chinese Dai in Xishuangbanna, China;
192 CDX) and the other including Japanese in Tokyo (JPT) from 1000 Genomes and NCBN
193 samples (Fig 2B). In addition, the latter cluster was divided into large and small clusters
194 consistent with the previous studies [7–9] in which the larger one was called the Hondo
195 population and the smaller one was called the Ryukyu population [7]. In this study, we
196 followed this convention (S1 Fig). The Hondo cluster consisted of 8,524 people, whereas
197 the Ryukyu cluster consisted of 182 people. We compared the allele frequencies of the
198 Japanese population (GEM Japan Whole-genome Aggregation) estimated based on the
199 WGS analysis in previous studies with those of the Hondo sample and found significant
200 frequency agreement (Fig 3A). While the allele frequencies between the Hondo and
201 Ryukyu populations also showed high agreement, the breadth of the distribution was wider

202 than the comparison between Hondo and GEM Japan (Fig 3B). This could be due to the
203 difference in the mainland and Ryukyu populations and the subsequent genetic drift.

204 Functional landscape of variants

205 The variants identified by WGS analysis were annotated for their biological functions. The
206 impact of the variants was classified based on the criteria of the annotation software and the
207 database as described in the Methods section. Deleterious mutations are more likely to be
208 kept at low frequencies in the population, as such mutations are less likely to spread in the
209 population because of negative selection. In fact, variants with a high impact on annotation
210 showed a clear tendency to have a low frequency in the population. The LOFTEE plugin of
211 Variant Effect Predictor was used to detect loss-of-function (LoF) variants in the Hondo
212 and Ryukyu populations. For comparison, we also detected LoF variants in 26 populations
213 in the 1000 Genomes Project phase 3 dataset [10]. 14,145 SNVs and 16,823 INDELs were
214 detected as high confident LoF specific to the Hondo population. For the Ryukyu
215 population, 211 SNVs and 288 INDELs were detected. The vast majority of LoF SNVs
216 exhibited a very low frequency in the Hondo population (Fig 4A). In fact, 76.0% of these
217 SNVs exhibited allele frequencies below 0.01%. We compared the number of LoF alleles
218 and the number of homozygous of LoF alleles per individual for Hondo, Ryukyu, and
219 populations in the 1000 Genomes Project (Fig 4 B and C, S2 Fig). Since homozygous LoFs
220 result in a complete loss of gene function, the number of homozygous LoFs in an
221 individual's genome can be used to measure the individual's genetic burden. Both indices
222 were highest in Africa, lowest in West Eurasia, and moderate in Hondo and Ryukyu. The

223 number of homozygous LoF alleles per individual by allele frequency was generally higher
224 in Africa across all allele frequencies (Fig 4D), which is consistent with the trend observed
225 in a previous study [11].

226 We compared the variants of NCBN samples with ClinVar registered variants [12]. A total
227 of 103,833 variants found in the Hondo population are registered in ClinVar. Of these,
228 2,427 were classified as "pathogenic" or "likely pathogenic" variants. Seven variants were
229 found in the four-star category, the most reliable classification based on the ClinVar review
230 status. Only one of them was "pathogenic" and a singleton variant (i.e., heterozygous in a
231 person) of the CTFR gene. The remaining six were polymorphic variants related to drug
232 responsiveness of CYP2C19. There were 1,130 variants in the 3-star category reviewed by
233 the expert panel. Of these, 56 were "pathogenic," and 13 were "likely pathogenic." The
234 frequencies of these variants were the highest, at 1.0%, and most of them were extremely
235 rare; only a few were observed in the population. Most of the less well-reviewed variants
236 with <3 stars had frequencies of less than 1%, but 34 variants had a frequency of 1% or
237 more.

238 Allele frequency estimation of HLA loci

239 Three-field HLA calling results from the WGS dataset in the present study were compared
240 with HLA allele frequencies HLA Foundation Laboratory (Kyoto, Japan) (S3 Fig). All
241 common HLA alleles (frequencies >1%) were concordant between the two datasets with
242 observed differences of less than 1%. To further validate our HLA calling results, a subset
243 of 94 samples was subjected to high-resolution HLA genotyping. Three-field HLA class I

244 (HLA-A, -C, and -B) accuracies were 96.3%, 97.9%, and 96.8%, respectively, and 3-field
245 HLA class II (HLA-DRB1, -DQA1, -DPA1, and -DPB1) accuracies were 98.9%, 100.0%,
246 98.9%, 100.0%, and 96.8%, respectively. The accuracy of 2-field HLA class I (HLA-A, -C,
247 and -B) increased to 97.9%, 98.4%, and 97.3%, respectively.

248 Evolutionary perspective of genomic diversity

249 The recent decrease in population size was detected in Hondo and Ryukyu populations.
250 Figure 5A shows the population histories of Hondo and Ryukyu populations inferred using
251 IBDNe [13], which estimated the changes in population size in recent (~200 generations
252 ago) past based on IBD sharing among individuals. In Hondo, the population size decreased
253 from about 75 to 50 generations ago, and from 17 to 11 generations ago. In the Ryukyu
254 population, a reduction in population size was observed from about 100 to 25 generations
255 ago. The distributions of IBD length were multimodal in both populations, indicating
256 fluctuations in population size (Fig 5B and 5C). We also estimated the long-term changes
257 in the effective population size from the genome-wide genealogy using Relate software
258 [14]. We estimated genome-wide genealogy based on the whole-genome data of 1,000
259 randomly selected samples from Hondo, 182 samples from the Ryukyu, and the CHB
260 population from the 1000 Genomes Project. The Ryukyu population showed a bottleneck
261 that peaked around 2,700 years ago (S4 Fig). Hondo/CHB population and Ryukyu
262 population diverged around 3,700 years ago, consistent with previous estimations of the
263 divergence time using SNP arrays [15,16].

264 We detected positive natural selection based on genome-wide genealogy of 1,000 Hondo
265 samples and found SNPs with p-values below the genome-wide significance level ($p < 5.0$
266 $\times 10^{-8}$) (S5 Fig, S2 Table). As the QQ plot suggested inflation of the test statistics (S6 Fig),
267 it is possible that the results contain false positives. However, the genes reported in
268 previous studies, which may have undergone positive natural selection, were correctly
269 included in the results. It is therefore important to consider this when interpreting the
270 results. For example, ALDH2 rs671 G/A (p-value = 2.0×10^{-17}) and ADH1B rs1229984
271 T/C (p-value = 6.8×10^{-10}), which are associated with alcohol metabolism, showed positive
272 natural selection signals [17,18]. The genealogies of the genes showed that the derived
273 alleles were spreading rapidly through the population (S7 Fig). The second example is
274 signals of positive natural selection on the non-synonymous rs76930569 C/T (p-value = 1.1
275 $\times 10^{-12}$) variant in the OCA2 gene. This variant is in complete linkage equilibrium with
276 rs1800414 T/C, involved in melanin biosynthesis, and has been shown to be associated
277 with light skin color and tanning ability in Asian populations [19–21]. The third example of
278 the positive selection is the FADS gene family. Multiple SNPs (rs174599, rs174600,
279 rs174601, rs97384, rs57535397, rs76996928) showed the signatures of positive selection.
280 FADS1 and FADS2 encode catalytic proteins, which synthesize long-chain fatty acids from
281 short-chain fatty acids [22], and have been subjected to natural selection related to diet in
282 several human populations [22–26]. We further analyzed change in allele frequency with
283 time for these genes under positive natural selection. We used CLUES software [27] to
284 estimate the allele frequency trajectory of SNPs in ALDH2, ADH1B, OCA2, and the
285 FADS gene family. The frequency of the derived alleles in ADH1B rs1229984 increased

286 about 20,000 years ago (Fig 6A). In contrast, the frequency of ALDH2 rs671 increased
287 from about 7,500 years ago (Fig 6B). The allele frequency trajectory of OCA2 rs1800414
288 (Fig 6C) showed that the frequency of derived allele of OCA2 rs1800414 began to increase
289 due to natural selection around 25,000 years ago. The frequency of derived allele of
290 rs174599 began increasing around 25,000 years ago, slowed down 15,000 years ago, and
291 started increasing again 10,000 years ago (Fig 6D).

292 Discussion

293 In the present study, we conducted a WGS analysis of samples from five biobanks in Japan.
294 Although the data obtained in this study are intended to be provided as control data for
295 genomic studies of various diseases, the analysis in this study focused on data quality and
296 population genetics properties. A uniform quality of data was obtained through the use of a
297 single procedure that encompassed both sequencing and data analysis. Population-based
298 studies using WGS analysis have been conducted in various populations [5,28,29]. Studies
299 on Japanese populations have already been reported [28], and the allele frequency
300 distributions in previous studies are consistent with the results of the present study (Fig
301 3A). The samples analyzed in the present study were provided by biobanks in three regions
302 of Japan: NCGM, NCCHD, and NCNP in the Tokyo area; NCGG in Aichi Prefecture in the
303 central area in the Honshu Island; and NCVC in Osaka Prefecture in the western area in
304 Honshu Island. Therefore, the genomic information obtained in the present study is
305 expected to reflect the regional diversity of Japan to some extent. For instance, the

306 population genetic analysis identified two clusters representing the ancestry of Ryukyu
307 Islands, comprising Okinawa Prefecture and the islands of Kagoshima Prefecture and the
308 Hondo region (mainland). This supports the idea that the Hondo and Ryukyu populations
309 are genetically differentiated, as suggested by anthropological studies [7–9]. We further
310 found that past population sizes differed between Hondo and Ryukyu. There was a
311 reduction in the Hondo population from 17 to 11 generations ago (Fig 5A). The
312 corresponding period was 476 and 308 years ago, and the assumption is that each
313 generation spanned 28 years; most of this duration overlaps with the Edo period in Japan.
314 This is consistent with findings from historical demography studies, which suggest that the
315 population not only increased but also remained stagnant due to limited economic growth,
316 population concentration in cities, and famine caused by cold weather-related damage
317 during this period. In contrast, the Ryukyu populations showed population reduction from
318 100 generations ago to 25 generations ago but then increased until the present (Fig 5A).
319 This population growth about 700 years ago was close to the beginning of farming in the
320 Ryukyu Islands (12th century). Assuming that agriculture was brought to the Ryukyu
321 Islands by migrants from the mainland of Japan, the population decline observed in the
322 Ryukyu population can be considered a bottleneck associated with the migration. The
323 population size estimated from the modern genome reflects the past population of the
324 migrants and should be influenced negligibly by the genetic diversity of the original
325 inhabitants of the Ryukyu Islands. Indeed, although the several human skeletal remains
326 have been discovered from Pleistocene sites in Ryukyu Islands [30,31], the previous
327 population genetic analysis based on genome-wide SNPs suggested minor genetic

328 contribution of the Pleistocene Ryukyu Island population to the modern Ryukyu population
329 [15,16]. The estimated time of divergence between Hondo/CHB and Ryukyu was 3,700
330 years ago (S4 Fig), suggesting that migration to the Ryukyu Islands occurred recently.

331 Studies of rare genetic diseases require data on the frequency of variants in the population.
332 Most of the variants we found in this study were rare, and many of them were newly
333 discovered in this study, as expected from population genetics theory. However, the lower
334 the frequency of the variants, the more difficult it becomes to distinguish them from errors.
335 In this study, we evaluated the accuracy of genotype detection, estimating a discordance
336 rate of 0.063% compared to genotype detection using WGS and SNP arrays. However, this
337 is an overestimation of the error rate due to the combined error of both technologies. We
338 also used the data obtained from the WGS analysis of the trio for validation. We estimated
339 the Mendelian error rate, which is the proportion of genotypes detected in the offspring of a
340 trio that is inconsistent with Mendel's laws of heredity. This method has the advantage of
341 being able to examine the entire genome compared to the use of SNP arrays. We found that
342 the Mendelian error rate is much higher for novel variants, i.e., previously reported
343 variants. The Mendelian error rate for novel SNVs was 2.26%, much higher than that of the
344 known SNVs (0.09%). This has important implications for the identification of causative
345 mutations in rare genetic diseases, as many causative mutations for these conditions are
346 newly discovered rare variants. This means that the discovery of such pathological variants
347 in patient sequencing is subject to a non-negligible degree of error.

348 We conducted the functional annotation of the variants discovered in this study. Consistent
349 with previous studies [5,28,29], variants that were expected to have a high biological
350 impact were less common in the population, confirming that negative natural selection
351 shapes the diversity of variants. Most of the LoF mutations were extremely rare, and most
352 of them were heterozygous (Fig 4A). The number of LoF mutations in the genome was
353 comparable to that in other Eurasian populations (Fig 4B). Although the Ryukyu population
354 has experienced population decline (Fig 5A), the frequency of LoF variants was
355 comparable to that in the Hondo population, and no evidence of differences in the profile of
356 rare functional variants due to the bottleneck effect was noted. The number of LoF sites and
357 homozygous LoF per individual in this study were higher than those detected in a previous
358 study [32]. Among these, the number of stop gained SNVs was consistent with that
359 recorded in the previous study [32], whereas the number of splice site SNVs and frameshift
360 INDELs was higher than that in the previous study [32] (S2 Fig). The number of LoF sites
361 was generally consistent with the number of LoF sites before manual curation in a previous
362 study [33]; thus, it may be possible to remove false-positive homozygous LoFs through
363 manual filtering, as in the previous study [33].

364 We also examined pathogenic variants that have been reported in the past. Pathogenic
365 variants assessed by an expert panel (4-star status) on ClinVar were found only in one to a
366 few individuals in the population. On the other hand, some variants that were less reviewed
367 were polymorphic with high frequency. These results reinforce the importance of utilizing
368 the frequency of the variants in the population to evaluate their pathogenicity.

369 Genes that have undergone positive natural selection in the East Asian populations are
370 related to the metabolism. This study supported that the dietary changes in the ancestors
371 seem to have shaped gene frequencies. Candidate regions undergoing positive natural
372 selection were found on a genome-wide scale using genealogy analysis (S5 Fig). ADH1B is
373 involved in metabolizing alcohol to acetaldehyde, and ALDH2 is involved in metabolizing
374 acetaldehyde. Both the non-synonymous A allele of ALDH2 rs671 and the C allele of
375 ADH1B rs1229984 affect the retention of acetaldehyde in the body and cause alcohol flush
376 in Asians [17,18]. These alleles have been suggested to be associated with Japanese dietary
377 habits and diseases, such as esophageal cancer [34,35]. Previous studies have hypothesized
378 that positive selection may have acted to maintain acetaldehyde in the blood against
379 parasite infection, which correlates with large-scale rice cultivation [36–39]. We also
380 observed that the increase in the frequency of ADH1B occurred earlier than that of
381 ALDH2, indicating that positive selection began to act at different times for these two
382 genes (Fig 6A and 6B). Based on the geographic distribution of haplotype structures around
383 ADH1B and ALDH2, according to Koganebuchi et al., positive selection on ADH1B
384 rs1229984 started before the beginning of the Jomon period, while positive natural
385 selection on ALDH2 began around 8,000 years ago, in association with the beginning of
386 rice cultivation in China [39]. Our dating by genome-wide genealogy of the Japanese
387 population genome is consistent with the above consideration. Using HapMap data, OCA2
388 rs1800414 has been shown in previous studies to be the effect of positive natural selection
389 on East Asians [19]. For the OCA2 gene, positive natural selection signals were found in
390 the European population for skin color-related SNPs other than those detected in this study

391 [19]. As natural selection works for light skin color, a previous study mentioned that it
392 enhances vitamin D synthesis capacity in regions with low sunlight [20]. For East Asians as
393 well, positive natural selection may have operated in relation to vitamin D synthesis in
394 regions with low sunlight. However, since the derived allele of rs1800414 is not necessarily
395 more frequent at the high latitudes of East Asia, other possibilities, such as sexual selection,
396 cannot be ruled out at this time [19]. The derived allele of rs1800414 has been shown to be
397 associated with light skin color and tanning ability in Chinese and Japanese populations
398 [20,21] and is widely observed in modern East Asians [19], suggesting that the derived
399 allele of rs1800414 originated in the common ancestor of East Asians and spread
400 throughout East Asia at very early stages of the East Asian population history. We
401 estimated that the derived allele of OCA2 rs1800414 began to increase in frequency around
402 25,000 years ago (Fig 6C). Future analyses of older East Asian lineages, such as the ancient
403 genome of the Jomon people, may reveal the original variant of this allele that led to
404 positive natural selection. FADS1 and FADS2 participate in fatty acid metabolism. For
405 example, in the Inuit population, which relies heavily on a marine animal diet, there are
406 positive natural selection signals on SNPs of FADS2 genes, which are responsible for the
407 increase in the concentrations of short-chain fatty acids [40]. Signals of positive natural
408 selection on alleles that promote long-chain fatty acid synthesis have also been identified in
409 African [22], European [25,26,41], and South Asian populations [24]. In particular, studies
410 in European populations have shown that the derived alleles of rs174594 and rs1714546 are
411 associated with increased total cholesterol and LDL cholesterol levels, increased expression
412 of FADS2, and decreased expression of FADS1 [25]. In European populations, increased

413 reliance on plant diets seemed to have resulted in positive natural selection on alleles that
414 promote long-chain fatty acid synthesis pathways of the FADS gene family [23,25,26]. The
415 SNPs in the FADS gene family detected in this study were associated with total cholesterol
416 and LDL cholesterol levels, increased expression of FADS2, and decreased expression of
417 FADS1 (S3 Table), like the SNPs subjected to natural selection in the European population
418 (S3 Table). These results suggest that in Hondo populations, as in Europeans, the dietary
419 change was accompanied by positive natural selection for alleles that promote the long-
420 chain fatty acid synthesis. The frequency of the derived allele of rs174599 in FADS2 began
421 to increase around 25,000 years ago, but the increase was not continuous, and there was a
422 period of stagnation from 15,000 years ago for 5,000 years (Fig 6D). Interestingly, the
423 frequency of this allele varies widely among East Asian populations. The derived allele was
424 major in CHB (64%) and Japanese (63%), whereas it was minor in Dai (Chinese Dai in
425 Xishuangbanna, China) (22%), Han Chinese in South (42%), and Kinh Vietnamese (20%);
426 these data suggest that the positive natural selection of the FADS gene family in East
427 Asians may reflect the association with agriculture and the complex dietary differences
428 among regional populations. Notably, Mathieson and Mathieson (2018) disproved the
429 simple idea that these derived alleles underwent positive natural selection in relation to the
430 introduction of agriculture and speculated that there were complex underlying factors, such
431 as unknown dietary changes [26].

432 In this study, we demonstrated that the data presented here can be used as a foundation for
433 analysis of human genetics. While this study focused on population genetic characterization
434 of the Japanese population, the data can be used in disease studies, as a resource for

435 genotype imputation in studies of common diseases, and as a control in studies on rare
436 diseases.

437 Materials and Methods

438 Sample preparation

439 DNA samples stored in the biobanks of five national centers (National Cerebral and
440 Cardiovascular Center; NCVC, National Center for Geriatrics and Gerontology; NCGG,
441 National Center for Global Health and Medicine; NCGM, National Center of Neurology
442 and Psychiatry; NCNP and National Center for Child Health and Development; NCCHD)
443 were submitted for WGS analysis. Samples derived from healthy individuals or patients
444 with some common diseases were selected as control groups for future disease studies. This
445 study was conducted with approval from the ethics review committee of the NCGM.
446 Informed consent for the analysis of these samples was received from all subjects in each
447 biobank. Approximately 50 µl of DNA at a concentration of 80 ng/µl per sample was
448 aliquoted into 96-well plates and shipped to an outsourced laboratory (TakaraBio, Shiga,
449 Japan) for WGS analysis.

450 WGS

451 To avoid quality fluctuations and batch effects, all samples were analyzed by a single
452 outsourced laboratory. WGS analysis was performed using NovaSeq6000 (Illumina, San
453 Diego, CA, US), and sample preparation was performed using the procedures and reagents

454 recommended by the manufacturer. DNA molecules were sonicated with a protocol
455 targeting an average size of 550 bp. DNA libraries were prepared using the TruSeq DNA
456 PCR-Free HT Library Prep Kit, and index sequences were added for multiplex analysis.
457 The insert size was confirmed by electrophoresis in the range of 400–750 bp before
458 sequencing runs. WGS was performed at 150 bp paired-end and repeated in multiplex until
459 an output of >90 Gbases without duplicated reads was obtained.

460 Data analysis

461 We received the quality controlled FASTQ data from the outsourced laboratory and
462 performed mapping and variant calling in an in-house data analysis pipeline. The mapping
463 and variant calls were performed using the Parabricks v3.1.0 (Nvidia, Santa Clara, CA,
464 US), which provides the capability to perform the analysis recommended by GATK at high
465 speed using a GPU [42]. The GRCh38 was used as the reference sequence. The pipeline
466 used in this study implements algorithms equivalent to those of bwa (v0.7.15) [43] and
467 GATK (v4.1.0). We flagged duplicates from mapped reads but did not perform realignment
468 and base quality score recalibration to reduce the computational time. The mapped data
469 were outputted in BAM format and converted into CRAM format using samtools [44] to
470 reduce the file size. Variant calls were output in gVCF format for joint calling. QC metrics
471 were obtained to evaluate the quality of the analyzed data. The depth and map rate were
472 calculated using GATK's CollectWgsMetrics tool. These QC metrics were continuously
473 monitored throughout the analysis. The sex chromosomes were analyzed assuming both
474 male and female genders. Variant calls were performed for chromosome X in the diploid (-

475 ploidy 2) model for females and the monoploid (-ploidy 1) model for males. Variant calls
476 of the pseudoautosomal region were performed in the diploid model. Variants of
477 chromosome Y were called in the monoploid mode regardless of the sample's gender.
478 Finally, the appropriate gVCF file for each sex was used during joint calling. Data from the
479 high-coverage WGS analysis of 2,504 individuals of the International 1000 Genomes
480 Project phase 3 [10] were used as population references for this study. The CRAM files
481 reanalyzed using high depth WGS were downloaded from a public database, and variant
482 calls were performed with the protocol described in this study.

483 Integrated analyses

484 To properly estimate the frequencies of variants found after WGS in the population, we
485 integrated the gVCF files. The joint calling was conducted by combining samples from the
486 biobank of NCBN and samples from the International 1000 Genomes Project phase 3. For
487 the joint calling, we used the gVCFtyper program of the Sentieon package [45]. This
488 program produces results equivalent to those of GeomicsDBImport followed by
489 GenotypeGVCFs programs for the joint calling of GATK. To perform efficient
490 computation in a cluster computation environment, we divided the autosomes into 29
491 regions evenly. Each variant was scored using VQSR to filter the integrated VCF. The
492 VarCal and ApplyVarCal programs of the Sentieon package corresponding to GATK's
493 VariantRecalibrator and ApplyVQSR, respectively, were used for this process. The
494 HapMap and International 1000 Genomes Omni2.5 sites, the high-confidence SNPs of the
495 International 1000 Genomes Project, and the dbSNP151 sites were used as true, training,

496 and known datasets, respectively. Variants identified as PASS, which correspond to
497 filtering with 99.9% sensitivity, were used in subsequent analyses unless otherwise noted.
498 The INDELs in the present variant set were normalized by performing left align, and
499 multiallelic variants were split into multiple variant records using the norm subcommand in
500 bcftools [44].

501 Variant annotation

502 Variants were annotated with the Variant Effect Predictor v102 [46]. We ran the loftee
503 plugin to evaluate the effects of the LoF variants. For the other evaluation of the functional
504 effects, dbNSFP4.1 [47] was used to assign precomputed evaluation values to the variants.
505 The metrics used for the assignment included LRT, SIFT, MutationTaster, and Polyphen2.

506 Genotyping by SNP array

507 Using JaponicaArray [48], genome-wide genotyping was performed on a subset of samples
508 for comparison with WGS results. Ninety-four samples each from five biobanks were
509 analyzed using the residual DNA after WGS analysis. The analysis was performed by an
510 outsourced laboratory (Toshiba, Tokyo, Japan), and the raw data in CEL format was
511 received. Four samples were dropped from the genotyping due to a low call rate (<97%) in
512 the first step of genotyping. Clustering for SNP genotyping of variants was performed on
513 the data of 466 individuals using the Analysis Power Tools (ver. 2.10.2.2, Thermo Fisher
514 Scientific, MA, USA). The clustering results for each probes' intensity were classified
515 using the SNPolisher program bundled with the Analysis Power Tools, and the 639,508

516 SNPs classified as "Recommended" in autosomes were used for subsequent analyses. The
517 genotype concordance with WGS was estimated using the hap.py software. To compare the
518 positions for which probes were designed in the SNP array, SNVs with the same position as
519 the SNP array were extracted from the results of WGS analysis. The SNP array results were
520 used as true data and the WGS results as query data. The genotype discordance rate
521 between the SNP array and WGS was calculated by dividing the number of false positives
522 by 639,508, which is the total number of SNPs compared.

523 Allele frequency estimation

524 To calculate the accurate allele frequencies, the ancestry of the samples was estimated
525 using PCA. Variants were filtered under more stringent criteria for this purpose.
526 Individual's genotypes were considered no calls if they had a genotype quality (GQ) of less
527 than 20, a depth outside the range of 11 to 64, or if less than 25% of the reads supported the
528 minor allele for heterozygous calls. Then, sites with SNPs that had a VQSR filter of PASS,
529 a minor allele frequency of >1%, and a call rate of >95% were retained. The KING
530 program [49] selected samples of unrelated individuals in the third-degree kinship or more.
531 For this dataset, independent SNPs were extracted using PLINK1.9 [50] with "-indep-
532 pairwise 500 50 0.1", and PCA was performed to calculate the principal component values
533 for each sample using PLINK1.9 [50]. Clusters were identified visually on the scatter plot
534 of the first and second principal components.

535 Allele and genotype frequencies were estimated for each ancestry group and biobank. The
536 fill-tags plugin of bcftools was used for these calculations. To compare the allele

537 frequencies in the Japanese population, we downloaded the GEM Japan frequency panel
538 information from TogoVar. Since the GEM Japan panel only provides information in hg19
539 coordinates, we converted it to GRCh38 coordinates. We used GATK's LiftoverVcf
540 program for the conversion.

541 HLA analysis

542 Three-field HLA alleles calling was performed using HLA-HD v1.3.0 [51] based on IPD-
543 IMGT/HLA v3.43.0 [52]; a score based on the weighted read counts considering variations
544 in and outside of the domain for antigen presentation was calculated to select the most
545 suitable pair of alleles amongst the candidate HLA alleles. To validate the accuracies of
546 HLA calling from WGS, HLA allele frequency distribution was compared with the HLA
547 frequency dataset from HLA Foundation Laboratory (Kyoto, Japan). To evaluate the
548 accuracy of HLA calling from the WGS dataset, a subset of the samples (n = 94) was
549 subjected to high-resolution experimental HLA genotyping for eight HLA genes (HLA-A, -
550 C, -B, -DRB1, -DQA1, -DQB1, -DPA1, and -DPB1) using next-generation sequencing and
551 AllType assay (One Lambda, West Hills, CA, US). Experimental HLA genotyping was
552 carried out following the vendor instructions, which consist of HLA gene amplification,
553 HLA library preparation, HLA template preparation, and HLA library loading onto an ion
554 530v1 chip (Thermo Fisher Scientific) in the Ion Chef (Thermo Fisher Scientific), followed
555 by final sequencing on the Ion S5 machine (Thermo Fisher Scientific). HLA genotype
556 assignments were carried out using HLATypeStream Visual (TSV v2.0; One Lambda,
557 West Hills, CA, US) and NGSengine® (v2.18.0.17625, GenDX, Utrecht, the Netherlands).

558 ## Haplotype phasing

559 Variant phasing was performed using shapeit v4.2 [53] in a haplotype-based analysis. SNPs
560 of unrelated samples identified using the ancestry inference were extracted for phasing. The
561 variant phasing was performed by dividing the autosomes into regions containing overlaps
562 for efficient computation. Each region was about 10 Mb in length, with a 500 kb overlap
563 margin at both ends. After phasing, VCFs were concatenated using the concat subcommand
564 in bcftools.

565 ## Estimation of recent population size change

566 We estimated the effective population size change of the Japanese population from IBD
567 sharing, which can estimate the population size change in the recent past (~200 generations
568 ago) using WGS data [13]. Population size change was estimated for each population based
569 on the whole-genome data of Hondo (8,524 individuals) and Ryukyu (182 individuals).
570 First, the hapibd software [54] was used to detect the IBD segments shared by each
571 individual. For the genetic distance, we referred to the HapMap genetic map data
572 distributed with hapibd. We then estimated the population size change of the Hondo and
573 Ryukyu populations using IBDNe (ibdne.23Apr20.ae9.jar). The shortest threshold of the
574 IBD segment length was set at 2 cM.

575 ## Estimation of genome-wide genealogy, estimation of population
576 size change, and detection of positive natural selection

577 We conducted the analysis of gene genealogy using the Relate software [14] to detect long-
578 term population size change and positive natural selection in Hondo and Ryukyu
579 populations. Relate is a software that can estimate genealogy on a genome-wide scale for
580 over 10,000 samples [55]. In this study, we used 1,000 randomly selected individual
581 genomes of Hondo, 182 Ryukyu samples, and 103 CHB samples of 1000 Genomes Project
582 [10]. First, input files (.haps, .samples) were created from vcf files using the
583 PrepareInputFiles.sh script in Relate software. We retrieved the Homo sapiens ancestral
584 sequences (GRCh38) of Ensembl 103 for the ancestral sequence and StrictMask of 1000
585 Genomes Project for genomic mask. Next, genome-wide genealogy was estimated using
586 the "Relate" command of Relate software packages. The mutation rate was set to $1.25 \times 10^{-}$
587 ^{8} per base per generation and the effective population size was set to 30,000. We assumed
588 28 years as the generation time in humans. The estimated genome-wide genealogy
589 (.anc, .mut) was used as input for population size estimation of Hondo and Ryukyu
590 populations using the EstimatePopulationSize.sh script. This script simultaneously
591 conducts estimation of population sizes, re-estimation of branch lengths using the estimated
592 population sizes, and estimation an average mutation rate. Finally, based on genome-wide
593 genealogy, we detected the target SNPs of positive natural selection acting on Hondo and
594 Ryukyu populations. Relate calculates a p-value of each SNP for positive selection that
595 quantifies how quickly a mutation has spread in the population. The p-values were

596 calculated for each SNP using the DetectSelection.sh script using the output genealogies of
597 population size estimation (.anc, .mut). We evaluated the quality of each SNP by
598 "RelateSelection –mode Quality," and SNPs inferred to be inaccurate tree estimation were
599 excluded.

600 Estimating the allele frequency trajectory

601 Changes in the allele frequency through the time were estimated using CLUES to infer
602 allele frequency trajectories [27]. CLUES uses the genome-wide genealogy inferred by
603 Relate. First, the sampleBranchLengths.sh script implemented in Relate was used to
604 MCMC sample the gene trees for the focal SNPs. Then, using the sampled tree file (.timeb)
605 as input, we estimated the allele frequency trajectory using CLUES's inference.py
606 command. The coalescence rate estimated by Relate (.coal file) can be used as an input to
607 modify the population size change using the -coal option. In this study, we estimated the
608 allele frequency trajectory by focusing on ALDH2 rs671, ADH1B rs1229984, OCA2
609 rs1800414, and FADS2 rs174600 among the SNPs that showed signals of natural selection
610 in Relate.

611

612

613

614

615 # Acknowledgments

616 We thank the participants who provided biological samples for this study. We thank Ms.
617 Megumi Tatsumi, Ms. Haruna Kaneko, Ms. Ayumi Fujisawa, Ms. Mami Sasaki, Ms.
618 Yukiko Miyashita, and Ms. Chikako Kinjyo at NCNP Biobank; Ms. Sachiyo Ito at NCGG
619 Biobank; Dr. Satoshi Suzuki at NCGM Biobank; the personnel at NCVC Biobank; Ms.
620 Kazuyo Kawamura, Dr. Kumiko Yanagi, Dr. Saki Aoto, and Ms. Fuyuki Hasegawa at
621 NCCHD Biobank; and Ms. Akino Takase at NCBN Central Biobank for their contributions
622 to this study. We also thank Dr. Leo Speidel for discussion on the results of Relate analysis
623 and Dr. Osamu Ogasawara for the technical support for the development of secondary
624 analysis pipelines. Computations were partially performed on the NIG supercomputer at
625 ROIS National Institute of Genetics.

626 # Funding

627 This work was supported by the Japan Agency for Medical Research and Development
628 under Grant No. JP19kk0205012 to M.M. and K.T. and MEXT Grant-in-aid for Scientific
629 Research on Innovative Areas under Grant No. 18H05505 to Y.K.

630 # Author contributions

631 **Conceptualization:** Y.K., N.E., M.M. and T.K.

632 **Methodology:** Y.O., R.Mi., E.N., H.G., K.Hata., K.Hatt., A.I., H.I-U., T.Kana., T.Kant.,
633 R.Ma., M.N., K.O., M.S., A.T., H.T., T.T., A.U., H.W., S.Y., Y.G., Y.Mar., Y.Mat., and
634 S.N.

635 **Data Curation:** K.K., H.S. and K.M.

636 **Formal Analysis:** Y.K., Y.W., and S-S.K.

637 **Project Administration:** Y.G., Y.Mar., Y.Mat., S.N. and K.T.

638 **Writing – Original Draft Preparation:** Y.K., W.Y., Y.O. and T.K.

639 Y.K., N.E., M.M., and T.K. designed the study. Y.O., R.Mi., H.G., K.Hata., K.Hatt., A.I.,
640 H.I-U., T.Kana., T.Kant., R.Ma., M.N., K.O., M.S., A.T., H.T., T.T., A.U., H.W., S.Y.,
641 Y.G., Y.Mar., Y.Mat., and S.N. contributed to the whole-genome sequencing. Y.O., R.Mi.,
642 and E.N. contributed to the SNP genotyping. K.K., H.S., and K.M. contributed to the data
643 collection. Y.K., Y.W., and S-S.K. contributed to the data analysis. Y.G., Y.Mar., Y.Mat.,
644 S.N., and K.T. contributed to the management of biobank. Y.K., W.Y., Y.O., and T.K.
645 wrote the manuscript with input from all authors.

646 Supporting information

647 Supporting information includes seven figures and three tables.

Competing interests

The authors declare no competing interests.

Web resources

IGSR: The International Genome Sample Resource, https://www.internationalgenome.org

Hap.py, https://github.com/Illumina/hap.py

GEM Japan, https://www.amed.go.jp/en/aboutus/collaboration/ga4gh_gem_japan.html

TogoVar, https://togovar.biosciencedbc.jp/

GATK, https://gatk.broadinstitute.org/hc/en-us

HLA frequency dataset from HLA Foundation Laboratory (Kyoto, Japan), http://hla.or.jp/index.html

Homo sapiens ancestral sequences (GRCh38), ftp://ftp.ensembl.org/pub/current_fasta/ancestral_alleles/homo_sapiens_ancestor_GRCh38.tar.gz

dbSNP, https://www.ncbi.nlm.nih.gov/snp/

662 # Data and code availability

663 The allele and genotype frequency data are available in the NBDC human database;
664 Accession: hum0331. The raw genomic data are available upon request to corresponding
665 authors and will soon be shared on a computational infrastructure currently under
666 construction by the Japan Agency for Medical Research and Development.

667

668 # References

669 1. Turnbull C, Scott RH, Thomas E, Jones L, Murugaesu N, Pretty FB, et al. The
670 100 000 Genomes Project: bringing whole genome sequencing to the NHS. BMJ.
671 2018;361: k1687. doi: 10.1136/bmj.k1687.

672 2. Taliun D, Harris DN, Kessler MD, Carlson J, Szpiech ZA, Torres R, et al.
673 Sequencing of 53,831 diverse genomes from the NHLBI TOPMed Program. Nature.
674 2021;590: 290–299. doi: 10.1038/s41586-021-03205-y.

675 3. The 1000 Genomes Project Consortium. An integrated map of genetic variation from
676 1,092 human genomes. Nature. 2012;491: 56–65. doi: 10.1038/nature11632.

677 4. Fu W, O'Connor TD, Jun G, Kang HM, Abecasis G, Leal SM, et al. Analysis of
678 6,515 exomes reveals the recent origin of most human protein-coding variants.
679 Nature. 2013;493: 216–220. doi: 10.1038/nature11690.

680 5. The Genome of the Netherlands Consortium. Whole-genome sequence variation,
681 population structure and demographic history of the Dutch population. Nat Genet.
682 2014;46: 818–825. doi: 10.1038/ng.3021.

683 6. Nagasaki M, Yasuda J, Katsuoka F, Nariai N, Kojima K, Kawai Y, et al. Rare
684 variant discovery by deep whole-genome sequencing of 1,070 Japanese individuals.
685 Nat Commun. 2015;6: 8018. doi: 10.1038/ncomms9018.

686 7. Yamaguchi-Kabata Y, Nakazono K, Takahashi A, Saito S, Hosono N, Kubo M, et al.
687 Japanese population structure, based on SNP genotypes from 7003 individuals

688 compared to other ethnic groups: Effects on population-based association studies.
689 Am J Hum Genet. 2008;83: 445–456. doi: 10.1016/j.ajhg.2008.08.019.

690 8. Jinam T, Nishida N, Hirai M, Kawamura S, Oota H, Umetsu K, et al. The history of
691 human populations in the Japanese Archipelago inferred from genome-wide SNP
692 data with a special reference to the Ainu and the Ryukyuan populations. J Hum
693 Genet. 2012;57: 787–95. doi: 10.1038/jhg.2012.114.

694 9. Watanabe Y, Isshiki M, Ohashi J. Prefecture-level population structure of the
695 Japanese based on SNP genotypes of 11,069 individuals. J Hum Genet. 2021;66:
696 431–437. doi: 10.1038/s10038-020-00847-0.

697 10. Byrska-Bishop M, Evani US, Zhao X, Basile AO, Abel HJ, Regier AA, et al. High
698 coverage whole genome sequencing of the expanded 1000 Genomes Project cohort
699 including 602 trios. bioRxiv. 2021; 2021.02.06.430068. doi:
700 10.1101/2021.02.06.430068.

701 11. Lek M, Karczewski KJ, Minikel E V, Samocha KE, Banks E, Fennell T, et al.
702 Analysis of protein-coding genetic variation in 60,706 humans. Nature. 2016;536:
703 285–291. doi: 10.1038/nature19057.

704 12. Landrum MJ, Lee JM, Benson M, Brown G, Chao C, Chitipiralla S, et al. ClinVar:
705 public archive of interpretations of clinically relevant variants. Nucleic Acids Res.
706 2016;44: D862–D868. doi: 10.1093/nar/gkv1222.

707 13. Browning SR, Browning BL. Accurate non-parametric estimation of recent effective
708 population size from segments of identity by descent. Am J Hum Genet. 2015;97:
709 404–418. doi: 10.1016/j.ajhg.2015.07.012.

710 14. Speidel L, Forest M, Shi S, Myers SR. A method for genome-wide genealogy
711 estimation for thousands of samples. Nat Genet. 2019;51: 1321–1329. doi:
712 10.1038/s41588-019-0484-x.

713 15. Sato T, Nakagome S, Watanabe C, Yamaguchi K, Kawaguchi A, Koganebuchi K, et
714 al. Genome-wide SNP analysis reveals population structure and demographic history
715 of the Ryukyu islanders in the southern part of the Japanese Archipelago. Mol Biol
716 Evol. 2014;31: 2929–2940. doi: 10.1093/molbev/msu230.

717 16. Matsunami M, Koganebuchi K, Imamura M, Ishida H, Kimura R, Maeda S. Fine-
718 scale genetic structure and demographic history in the Miyako Islands of the Ryukyu
719 Archipelago. Mol Biol Evol. 2021;38: 2045–2056. doi: 10.1093/molbev/msab005.

720 17. Harada S, Agarwal DP, Goedde HW. Aldehyde dehydrogenase deficiency as cause
721 of facial flushing reaction to alcohol in Japanese. Lancet. 1981;2: 982. doi:
722 10.1016/s0140-6736(81)91172-7.

723 18. Edenberg HJ, McClintick JN. Alcohol dehydrogenases, aldehyde dehydrogenases,
724 and alcohol use disorders: A critical review. Alcohol Clin Exp Res. 2018;42: 2281–
725 2297. doi: 10.1111/acer.13904.

726 19. Donnelly MP, Paschou P, Grigorenko E, Gurwitz D, Barta C, Lu R-B, et al. A global
727 view of the OCA2-HERC2 region and pigmentation. Hum Genet. 2012;131: 683–
728 696. doi: 10.1007/s00439-011-1110-x.

729 20. Yang Z, Zhong H, Chen J, Zhang X, Zhang H, Luo X, et al. A genetic mechanism
730 for convergent skin lightening during recent human evolution. Mol Biol Evol.
731 2016;33: 1177–1187. doi: 10.1093/molbev/msw003.

732 21. Shido K, Kojima K, Yamasaki K, Hozawa A, Tamiya G, Ogishima S, et al.
733 Susceptibility loci for tanning ability in the Japanese population identified by a
734 genome-wide association study from the Tohoku Medical Megabank Project Cohort
735 Study. J Invest Dermatol. 2019;139: 1605-1608.e13. doi: 10.1016/j.jid.2019.01.015.

736 22. Mathias RA, Fu W, Akey JM, Ainsworth HC, Torgerson DG, Ruczinski I, et al.
737 Adaptive evolution of the FADS gene cluster within Africa. PLoS One. 2012;7:
738 e44926. doi: 10.1371/journal.pone.0044926.

739 23. Mathieson I, Lazaridis I, Rohland N, Mallick S, Patterson N, Roodenberg SA, et al.
740 Genome-wide patterns of selection in 230 ancient Eurasians. Nature. 2015;528: 499–
741 503. doi: 10.1038/nature16152.

742 24. Kothapalli KSD, Ye K, Gadgil MS, Carlson SE, O'Brien KO, Zhang JY, et al.
743 Positive selection on a regulatory insertion-deletion polymorphism in FADS2
744 influences apparent endogenous synthesis of arachidonic acid. Mol Biol Evol.
745 2016;33: 1726–1739. doi: 10.1093/molbev/msw049.

746 25. Buckley MT, Racimo F, Allentoft ME, Jensen MK, Jonsson A, Huang H, et al.
747 Selection in Europeans on fatty acid desaturases associated with dietary changes.
748 Mol Biol Evol. 2017;34: 1307–1318. doi: 10.1093/molbev/msx103.

749 26. Mathieson S, Mathieson I. FADS1 and the timing of human adaptation to
750 agriculture. Mol Biol Evol. 2018;35: 2957–2970. doi: 10.1093/molbev/msy180.

751 27. Stern AJ, Wilton PR, Nielsen R. An approximate full-likelihood method for inferring
752 selection and allele frequency trajectories from DNA sequence data. PLoS Genet.
753 2019;15: e1008384. doi: 10.1371/journal.pgen.1008384.

754 28. Nagasaki M, Yasuda J, Katsuoka F, Nariai N, Kojima K, Kawai Y, et al. Rare
755 variant discovery by deep whole-genome sequencing of 1,070 Japanese individuals.
756 Nat Commun. 2015;6: 8018. doi: 10.1038/ncomms9018.

757 29. Gudbjartsson DF, Helgason H, Gudjonsson SA, Zink F, Oddson A, Gylfason A, et
758 al. Large-scale whole-genome sequencing of the Icelandic population. Nat Genet.
759 2015;47: 435–444. doi: 10.1038/ng.3247.

760 30. Suzuki H. Discoveries of the fossil man from Okinawa Island. Anthropol Sci.
761 1975;83: 113–124. doi: 10.1537/ase1911.83.113.

762 31. Nakagawa R, Doi N, Nishioka Y, Nunami S, Yamauchi H, Fujita M, et al.
763 Pleistocene human remains from Shiraho-Saonetabaru Cave on Ishigaki Island,
764 Okinawa, Japan, and their radiocarbon dating. Anthropol Sci. 2010;118: 173–183.
765 doi: 10.1537/ase.091214.

766 32. MacArthur DG, Balasubramanian S, Frankish A, Huang N, Morris J, Walter K, et al.
767 A systematic survey of loss-of-function variants in human protein-coding genes.
768 Science. 2012;335: 823–828. doi: 10.1126/science.1215040.

769 33. Karczewski KJ, Francioli LC, Tiao G, Cummings BB, Alföldi J, Wang Q, et al. The
770 mutational constraint spectrum quantified from variation in 141,456 humans. Nature.
771 2020;581: 434–443. doi: 10.1038/s41586-020-2308-7.

772 34. Cui R, Kamatani Y, Takahashi A, Usami M, Hosono N, Kawaguchi T, et al.
773 Functional variants in ADH1B and ALDH2 coupled with alcohol and smoking
774 synergistically enhance esophageal cancer risk. Gastroenterology. 2009;137: 1768–
775 1775. doi: 10.1053/j.gastro.2009.07.070.

776 35. Matoba N, Akiyama M, Ishigaki K, Kanai M, Takahashi A, Momozawa Y, et al.
777 GWAS of 165,084 Japanese individuals identified nine loci associated with dietary
778 habits. Nat Hum Behav. 2020;4: 308–316. doi: 10.1038/s41562-019-0805-1.

779 36. Oota H, Pakstis AJ, Bonne-Tamir B, Goldman D, Grigorenko E, Kajuna SLB, et al.
780 The evolution and population genetics of the ALDH2 locus: random genetic
781 drift, selection, and low levels of recombination. Ann Hum Genet. 2004;68: 93–109.
782 doi: 10.1046/j.1529-8817.2003.00060.x.

783 37. Han Y, Gu S, Oota H, Osier M V, Pakstis AJ, Speed WC, et al. Evidence of positive
784 selection on a class I ADH locus. Am J Hum Genet. 2007;80: 441–456. doi:
785 10.1086/512485.

786 38. Luo H-R, Wu G-S, Pakstis AJ, Tong L, Oota H, Kidd KK, et al. Origin and dispersal
787 of atypical aldehyde dehydrogenase ALDH2∗487Lys. Gene. 2009;435: 96–103. doi:
788 10.1016/j.gene.2008.12.021.

789 39. Koganebuchi K, Haneji K, Toma T, Joh K, Soejima H, Fujimoto K, et al. The allele
790 frequency of ALDH2*Glu504Lys and ADH1B*Arg47His for the Ryukyu islanders
791 and their history of expansion among East Asians. Am J Hum Biol. 2017;29:
792 e22933. doi: 10.1002/ajhb.22933.

793 40. Fumagalli M, Moltke I, Grarup N, Racimo F, Bjerregaard P, Jørgensen ME, et al.
794 Greenlandic Inuit show genetic signatures of diet and climate adaptation. Science.
795 2015;349: 1343–1347. doi: 10.1126/science.aab2319.

796 41. Mallick S, Li H, Lipson M, Mathieson I, Gymrek M, Racimo F, et al. The Simons
797 Genome Diversity Project: 300 genomes from 142 diverse populations. Nature.
798 2016;538: 201–206. doi: 10.1038/nature18964.

799 42. Franke KR, Crowgey EL. Accelerating next generation sequencing data analysis: an
800 evaluation of optimized best practices for Genome Analysis Toolkit algorithms.
801 Genomics Inform. 2020;18: e10. doi: 10.5808/GI.2020.18.1.e10.

802 43. Li H, Durbin R. Fast and accurate short read alignment with Burrows–Wheeler
803 transform. Bioinformatics. 2009;25: 1754–1760. doi:
804 10.1093/bioinformatics/btp324.

805 44. Danecek P, Bonfield JK, Liddle J, Marshall J, Ohan V, Pollard MO, et al. Twelve
806 years of SAMtools and BCFtools. GigaScience. 2021;10: giab008. doi:
807 10.1093/gigascience/giab008.

808 45. Freed D, Aldana R, Weber JA, Edwards JS. The Sentieon Genomics Tools - A fast
809 and accurate solution to variant calling from next-generation sequence data. bioRxiv.
810 2017; 115717. doi: 10.1101/115717.

811 46. McLaren W, Gil L, Hunt SE, Riat HS, Ritchie GRS, Thormann A, et al. The
812 ensembl variant effect predictor. Genome Biol. 2016;17: 122. doi: 10.1186/s13059-
813 016-0974-4.

814 47. Liu X, Li C, Mou C, Dong Y, Tu Y. dbNSFP v4: a comprehensive database of
815 transcript-specific functional predictions and annotations for human nonsynonymous
816 and splice-site SNVs. Genome Med. 2020;12: 103. doi: 10.1186/s13073-020-00803-
817 9.

818 48. Kawai Y, Mimori T, Kojima K, Nariai N, Danjoh I, Saito R, et al. Japonica array:
819 improved genotype imputation by designing a population-specific SNP array with
820 1070 Japanese individuals. J Hum Genet. 2015;60: 581–587. doi:
821 10.1038/jhg.2015.68.

822 49. Manichaikul A, Mychaleckyj JC, Rich SS, Daly K, Sale M, Chen W-M. Robust
823 relationship inference in genome-wide association studies. Bioinformatics. 2010;26:
824 2867–2873. doi: 10.1093/bioinformatics/btq559.

825 50. Chang CC, Chow CC, Tellier LC, Vattikuti S, Purcell SM, Lee JJ. Second-
826 generation PLINK: rising to the challenge of larger and richer datasets. GigaScience.
827 2015;4: 7. doi: 10.1186/s13742-015-0047-8.

51. Kawaguchi S, Higasa K, Shimizu M, Yamada R, Matsuda F. HLA-HD: An accurate HLA typing algorithm for next-generation sequencing data. Hum Mutat. 2017;38: 788–797. doi: 10.1002/humu.23230.

52. Robinson J, Barker DJ, Georgiou X, Cooper MA, Flicek P, Marsh SGE. IPD-IMGT/HLA database. Nucleic Acids Res. 2020;48: D948–D955. doi: 10.1093/nar/gkz950.

53. Delaneau O, Zagury J-F, Robinson MR, Marchini JL, Dermitzakis ET. Accurate, scalable and integrative haplotype estimation. Nature Commun. 2019;10: 5436. doi: 10.1038/s41467-019-13225-y.

54. Zhou Y, Browning SR, Browning BL. A fast and simple method for detecting identity-by-descent segments in large-scale data. Am J Hum Genet. 2020;106: 426–437. doi: 10.1016/j.ajhg.2020.02.010.

55. Speidel L, Forest M, Shi S, Myers SR. A method for genome-wide genealogy estimation for thousands of samples. Nat Genet. 2019;51: 1321–1329. doi: 10.1038/s41588-019-0484-x.

853 # Figure legends

854 **Fig 1. Quality control metrics of whole-genome sequencing.** Quality control metrics for
855 each sample are plotted against the sample in the horizontal axis direction; QC indices are
856 (A) average coverage of reads in autosomal loci after excluding duplicated reads, (B)
857 mapping rate, and (C) average insert length. Saliva-derived samples are colored by yellow.

858 **Fig 2. Genetic structure of NCBN samples.** (A) The first and second principal
859 components are plotted. The continental population of the international 1000 genomes and
860 NCBN are plotted in different colors and shapes. (B) PCA plots of the East Asian
861 population of the International 1000 Genomes and NCBN samples are shown. JPT:
862 Japanese in Tokyo, Japan, CHB: Han Chinese in Beijing, China, CHS: Han Chinese South,
863 KHV: Kinh in Ho Chi Minh City, Vietnam, CDX: Chinese Dai in Xishuangbanna, China

864 **Fig 3. Comparison of allele frequency between different populations.** (A) The non-
865 reference allele frequencies of the Hondo population of NCBN samples (X-axis) and the
866 corresponding variants of GEM Japan (Y-axis) were counted and then the numbers were
867 plotted as density. (B) Same plot for Hondo population (X-axis) and Ryukyu population
868 (Y-axis).

869 **Fig 4. Analysis of loss-of-function (LoF) variants**. (A) The allele frequency distribution
870 of newly detected HC LoF SNPs in the Hondo population. (B) The number of LoF alleles
871 and (C) the number of homozygous of LoF alleles per individual for Hondo Ryukyu, and
872 populations of the International 1000 Genomes. (D) The number of homozygous of LoF

873 alleles per individual by allele frequency for Hondo, Ryukyu, and the populations of the
874 International 1000 Genomes.

875 **Fig 5. Estimation of past population size from IBD sharing.** (A) Short-term effective
876 population size change in Hondo and Ryukyu populations by IBDNe. (B) Distribution of
877 IBD segment length in Hondo. (C) Distribution of IBD segment length in Ryukyu.

878 **Fig 6. Trajectories of allele frequency of genes.** Allele frequency trajectories of (A)
879 ADH1B rs1229984, (B) ALDH2 rs671, (C) OCA2 rs1800414, and (D) FADS1 rs174599
880 are shown.

881

882

883

884

885

886

887

888

889

890 # Supporting information

891 **S1 Fig. Genetic structure of East Asian populations.** The clusters consisting of the
892 NCBN samples in Figure 2 are classified into Hondo (black), Ryukyu (orange), and others
893 (blue).

894 **S2 Fig. Analysis of Loss-of-function (LoF) variants.** The numbers of LoF sites per
895 individual by category are presented: (A) and (B) stop gained SNV; (C) and (D) splice site
896 SNV; (E) and (F) frameshift INDELs.

897 **S3 Fig. HLA alleles frequencies (%) between NCBN vs HLA Foundation Laboratory,**
898 **Kyoto, Japan.** Comparison for class I HLA genes (HLA-A, -C, -B) (left). Comparison for
899 class II HLA genes (HLA-DRB1, -DQA1, -DQB1, -DPA1, -DPB1) (right). Only common
900 HLA alleles (HLA frequencies > 1%) are included in this analysis.

901 **S4 Fig. Long-term effective population size change of Hondo, Ryukyu, and Han**
902 **Chinese.** The changes in population size were estimated from the gene genealogy across
903 the genome.

904 **S5 Fig. Manhattan plot of the selection scan result of the whole-genome SNPs by**
905 **Relate.** The red line represents the genome-wide significance level (5×10^{-8}).

906 **S6 Fig. QQ plot of the selection scan result of the whole-genome SNPs by Relate.** The
907 red line denotes y=x.

908 **S7 Fig. Gene genealogy estimated by Relate.** Genealogy of (a) ALDH2 rs671, (b)

909 ADH1B rs1229984 (c) OCA2 rs1800414 (d) FADS1 rs174599 are presented. The vertical

910 axis represents the age (years before present). Derived allele carriers are shown in red.

911

912

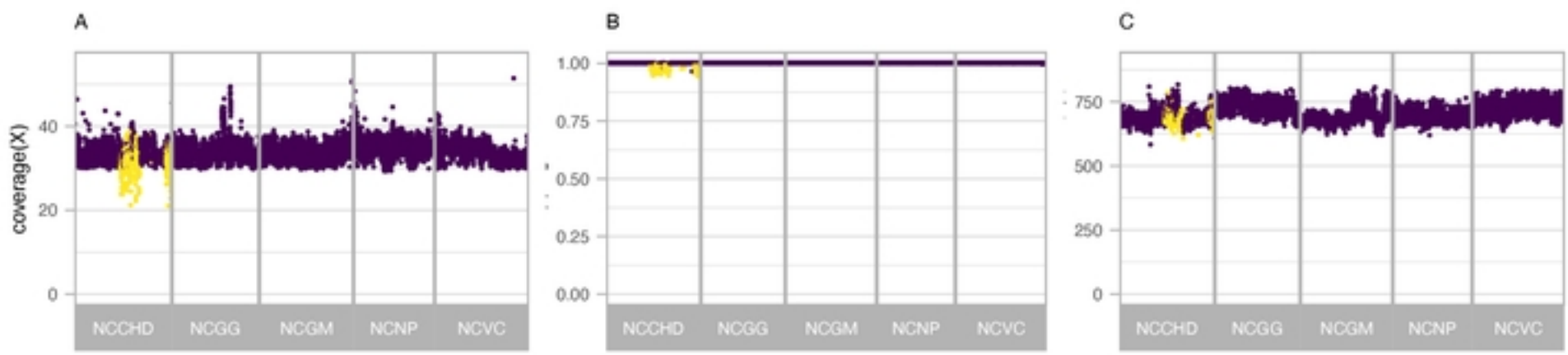
A
B
C
coverage(X)
40
20
0
1.00
0.75
0.50
0.25
0.00
750
500
250
0
NCCHD
NCGG
NCGM
NCNP
NCVC

Figure 1.

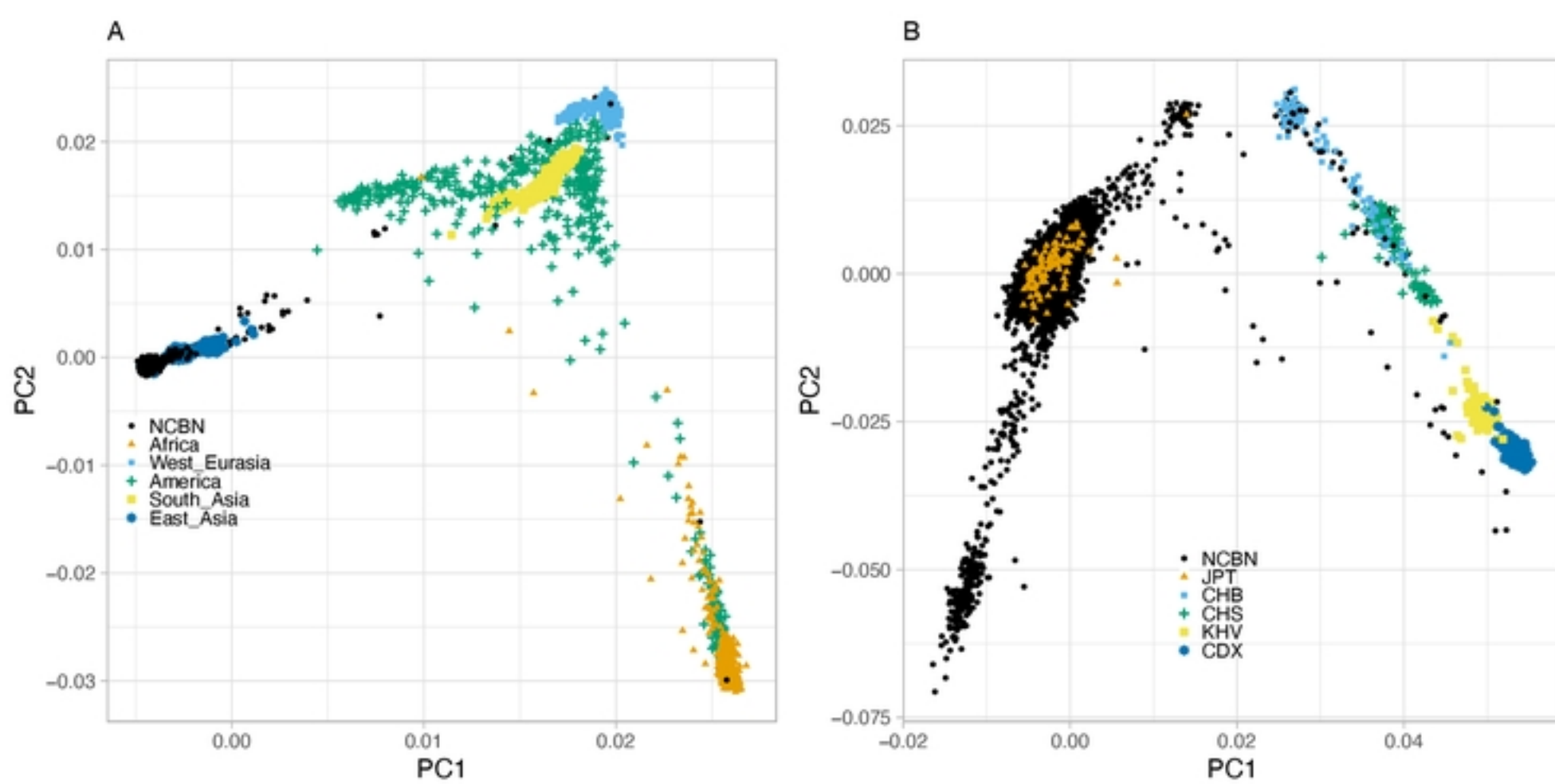
A
0.02
0.01
0.00
−0.01
−0.02
−0.03
PC2
0.00
0.01
0.02
PC1
NCBN
Africa
West_Eurasia
America
South_Asia
East_Asia
B
0.025
0.000
−0.025
−0.050
−0.075
PC2
−0.02
0.00
0.02
0.04
PC1
NCBN
JPT
CHB
CHS
KHV
CDX

Figure 2.

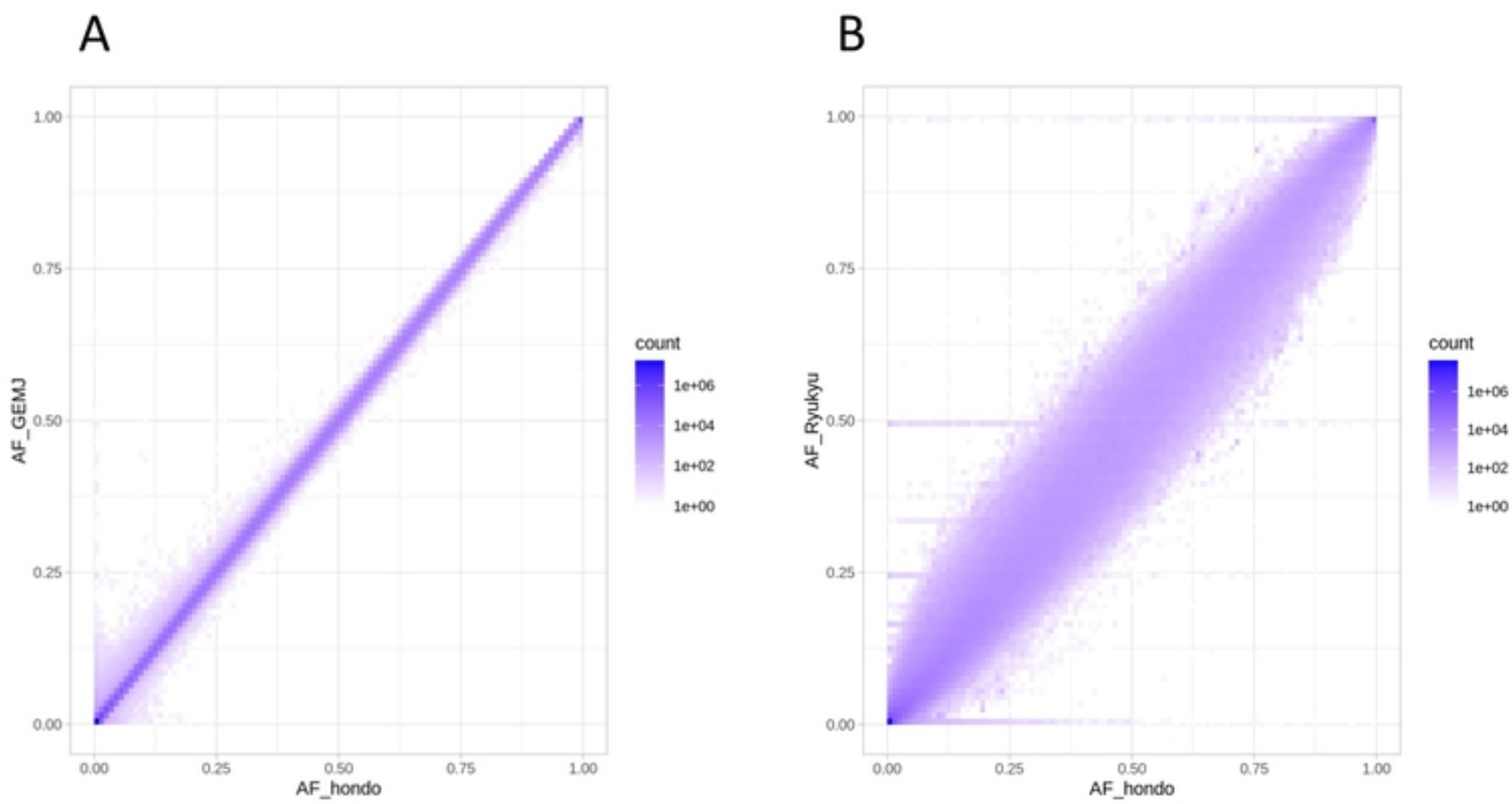
A
B
AF_GEMJ
AF_hondo
AF_Ryukyu
AF_hondo
count
1e+06
1e+04
1e+02
1e+00
0.00
0.25
0.50
0.75
1.00

Figure 3

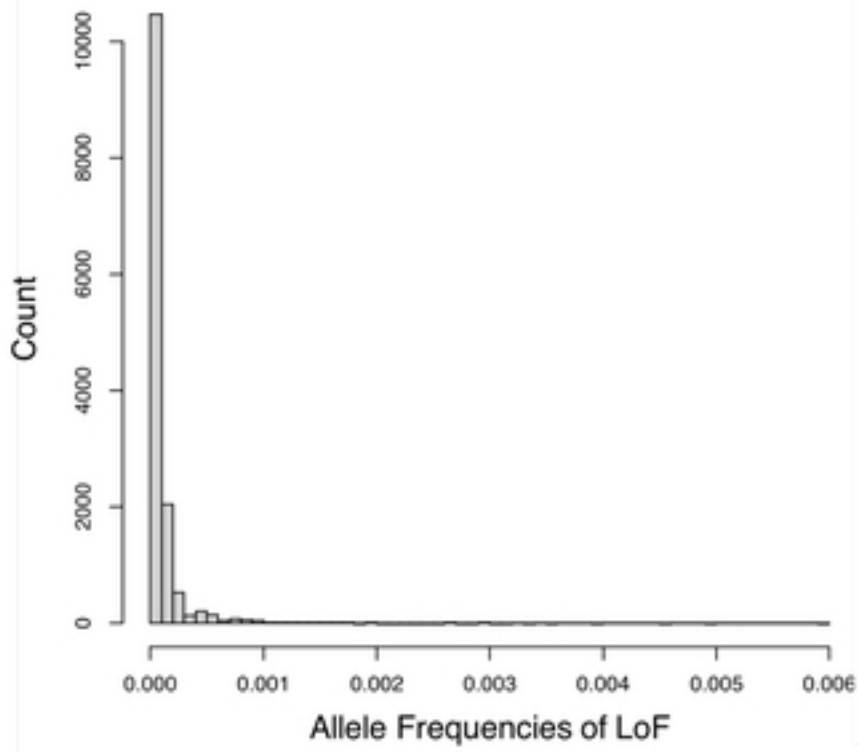
A
Count
Allele Frequencies of LoF

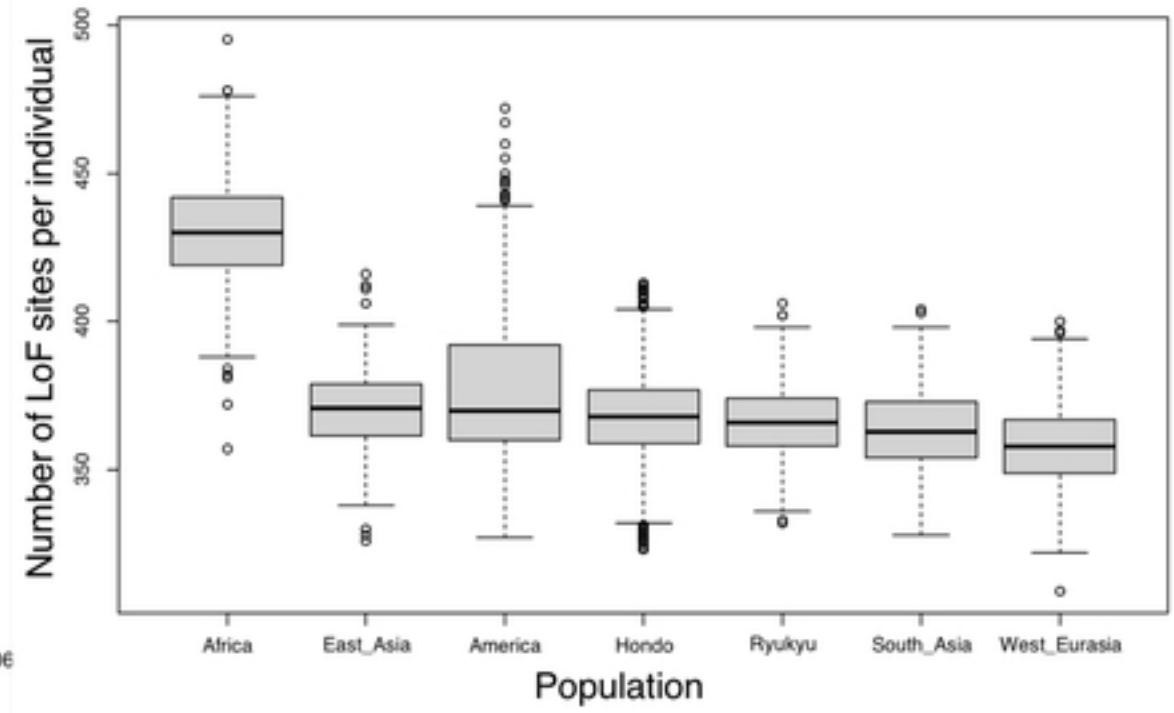
B
Number of LoF sites per individual
Africa
East_Asia
America
Hondo
Ryukyu
South_Asia
West_Eurasia
Population

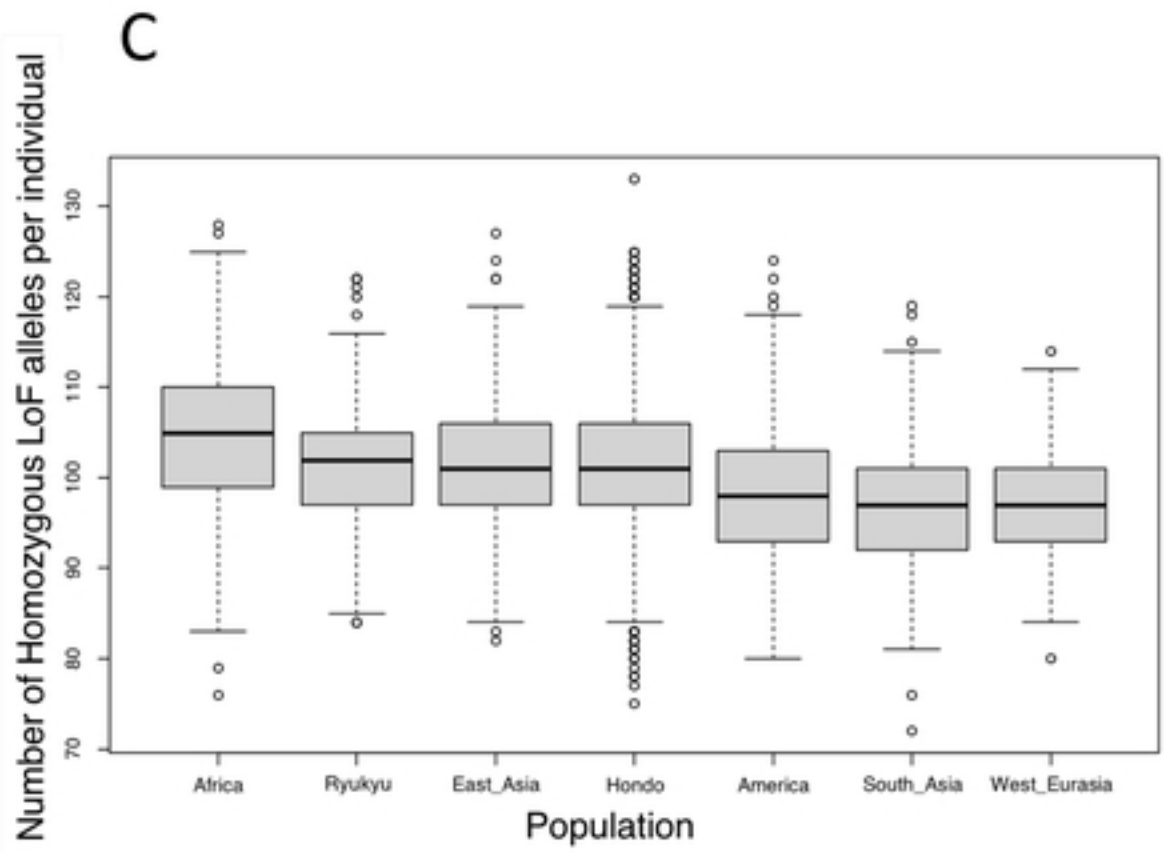
C
Number of Homozygous LoF alleles per individual
Africa
Ryukyu
East_Asia
Hondo
America
South_Asia
West_Eurasia
Population

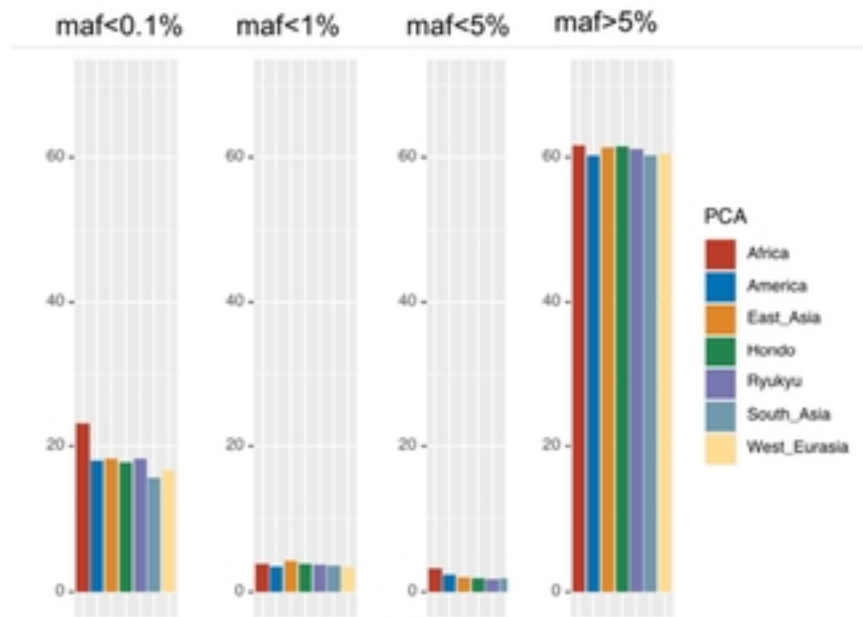
D
maf<0.1%
maf<1%
maf<5%
maf>5%
PCA
Africa
America
East_Asia
Hondo
Ryukyu
South_Asia
West_Eurasia

Figure 4

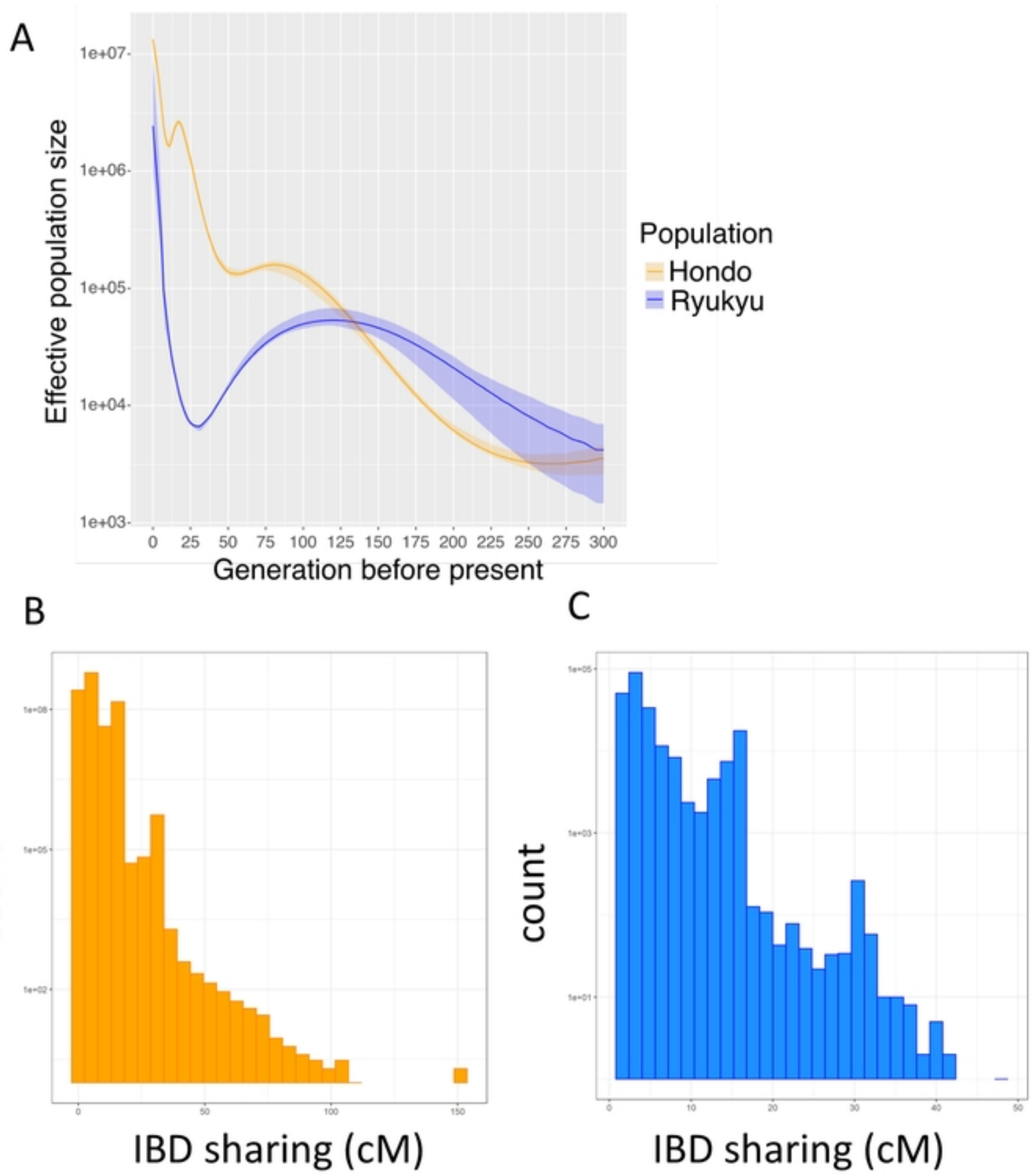
A
Effective population size
1e+07
1e+06
1e+05
1e+04
1e+03
0 25 50 75 100 125 150 175 200 225 250 275 300
Generation before present
Population
Hondo
Ryukyu
B
count
IBD sharing (cM)
C
count
IBD sharing (cM)

Figure 5

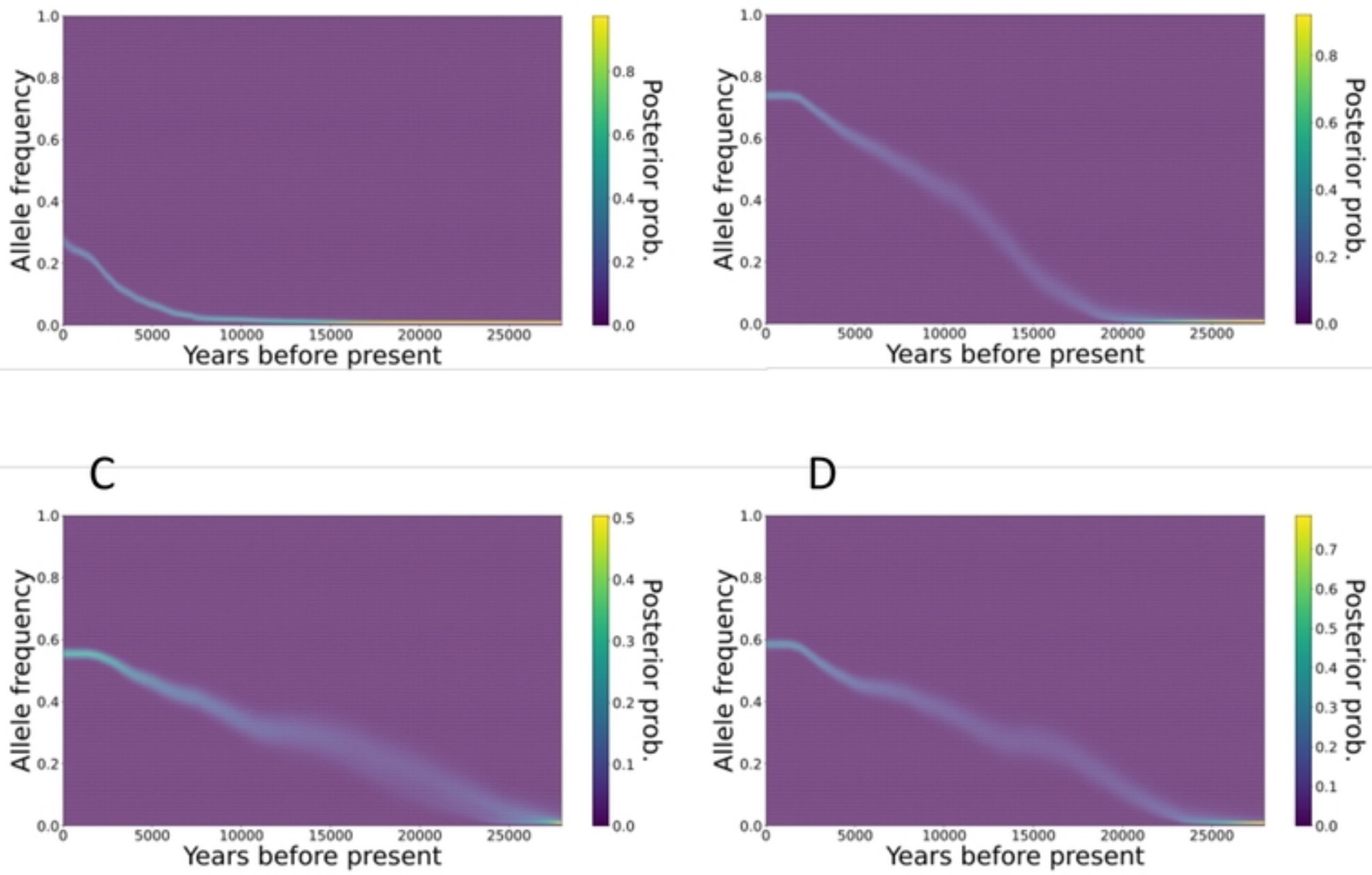
A
B
C
D
Allele frequency
Years before present
Posterior prob.

Figure 6